Relationship between the structure and optical properties of lithium tantalate at the zero-birefringence point

S. Huband, , D. S. Keeble, , N. Zhang, , A. M. Glazer, , A. Bartasyte, and , and P. A. Thomas

Citation: Journal of Applied Physics **121**, 024102 (2017); doi: 10.1063/1.4973685
View online: http://dx.doi.org/10.1063/1.4973685
View Table of Contents: http://aip.scitation.org/toc/jap/121/2
Published by the American Institute of Physics

Relationship between the structure and optical properties of lithium tantalate at the zero-birefringence point

S. Huband,[1,a)] D. S. Keeble,[1,2] N. Zhang,[3] A. M. Glazer,[1,4] A. Bartasyte,[5] and P. A. Thomas[1]
[1]*Department of Physics, University of Warwick, Coventry, West Midlands CV4 7AL, United Kingdom*
[2]*Diamond Light Source Ltd., Harwell Science and Innovation Campus, Chilton, Didcot, Oxfordshire OX11 ODE, United Kingdom*
[3]*Electronic Materials Research Laboratory, Key Laboratory of the Ministry of Education and International Center for Dielectric Research, Xi'an Jiaotong University, Xi'an 710049, People's Republic of China*
[4]*Clarendon Laboratory, University of Oxford, Parks Road, Oxford OX1 3PU, United Kingdom*
[5]*Institute FEMTO-ST, Université Bourgogne Franche-Comté, 26 rue de l'Epitaphe, 25030 Besançon, France*

(Received 25 October 2016; accepted 22 December 2016; published online 10 January 2017)

The structure of lithium tantalate powders has been investigated using neutron diffraction between room temperature and 445 K, which includes the zero-birefringence point. As the temperature increases, the displacement of the Ta atom from the centre of the O octahedra and the tilt of the octahedra both decrease linearly in the range investigated. The measured structures form the basis of a range of density functional theory calculations utilizing the WIEN2 k code, with a focus on calculating the optical properties. These calculations are sensitive to the small structural changes measured in this temperature range; the calculated birefringence changes are consistent with the changes measured experimentally. Further, by investigating the effect of each atom in isolation, it can be shown that the birefringence of lithium tantalate mainly depends on the Ta displacement and the octahedral tilt, with the linear change in these as a function of temperature producing the change in birefringence with temperature, which results in it becoming zero-birefringent. This work demonstrates the unique material insights that can be obtained by combining density functional calculations with precise structural studies. *Published by AIP Publishing.*
[http://dx.doi.org/10.1063/1.4973685]

I. INTRODUCTION

Lithium tantalate (LT) is an important material for electro-optic devices, and with lithium niobate (LN) it forms a solid solution $LiNb_{1-x}Ta_xO_3$ (LNT), which has been of interest for its room temperature zero-birefringence.[1–5] Despite its widespread use in devices, the relationship between the structure and some physical properties such as the birefringence, ferroelectricity, and paraelectric phase transition is not fully understood.[6,7] It is well known that LT can be made with a range of Li concentrations, with compositions ranging from 46 mol. % Li_2O to 50 mol. % Li_2O.[8–10] The birefringence has been investigated as a function of temperature between 48 and 50 mol. % Li_2O using vapor transport equilibrium (VTE) treated crystals, giving the temperature of the zero-birefringence point of stoichiometric LT as 373 K.[2] The birefringence of LNT crystals has also been investigated and for Li-deficient LNT crystals, a composition of 93–96 mol. % Ta is zero birefringent at room temperature.[1,3,11]

LN and LT are isostructural and ferroelectric with space group $R3c$ at room temperature and both undergo a high-temperature phase transition to the paraelectric space group $R\bar{3}c$. A set of parameters for rhombohedral perovskite structures such as LN and LT was introduced by Megaw to parameterize the structure using the cation positions, octahedral distortion, and octahedral tilt.[12] In this system, the O atom is held fixed at the first O plane (z = 1/12) allowing the position of the Ta atom to be determined by its displacement (t) along the c-axis from the origin, which is also the centre of the oxygen octahedra. The Li position is then given by its displacement (s) along the c-axis from the 12-coordinated site at z = 1/4 and the O x and y position by the octahedral distortion (d) and a displacement (e), which is related to the octahedral tilt ω by

$$\tan \omega = 4\sqrt{3e}. \quad (1)$$

The change in these parameters with increasing temperature was calculated for LN by Megaw using the powder X-ray diffraction (XRD) measurements of Abrahams *et al.*;[13] the octahedral tilt decreases with increasing temperature, resulting in an increase in the a lattice parameter.[14] The curve in the c lattice parameter as a function of temperature is explained by the decrease in the Nb displacement with increasing temperature. Above the Curie point, in the paraelectric phase, the Nb/Ta displacement and the octahedral distortion disappear, but the octahedral tilt remains.

A number of single-particle density functional theory (DFT) calculations on LT have been performed with a focus on calculating the band gap; Cabuk *et al* calculated a band gap of 3.86 eV using the local-density approximation (LDA), and Riefer *et al*. calculated a band gap of 3.71 eV using the generalized gradient approximation (GGA).[15,16] Recently, there has been a focus on the calculated band gap of LN and what the experimental value is,[17] and following this, it has

a)Author to whom correspondence should be addressed. Electronic mail: s.huband@warwick.ac.uk

been suggested that DFT calculations should be performed focusing on the well-known physical properties, such as the refractive index.[18] Riefer *et al*. made a series of calculations on LNT focusing on the birefringence, and the calculated values agreed closely with the measured values of Wood *et al*.[3] These calculations included self-energy effects and electron-hole interactions, which increased the calculated band gap of LT to 5.65 eV.

The present study aims at a better understanding of the structure and optical properties by using experimentally determined structures as the basis for single-particle DFT calculations. These measurements have been made between room temperature and 445 K with the expected zero-birefringence point of LT at 373 K. The use of powder neutron diffraction provides precise values for the lattice parameters as well as the Li, O, and Ta positions; this high precision then allows the small structural changes as a function of temperature to be investigated.

II. METHODOLOGY

A. Experimental

The LT powder sample was prepared by a solid-state reaction between Li_2CO_3 (99.99%) and Ta_2O_5 (99.85%), with the Li in Li_2CO_3 enriched to 99.9% ^{7}Li, following the method of Bartasyte *et al*.[19] The starting materials were weighed out with a stoichiometric ratio and ball-milled in isopropanol, sealed in a platinum crucible and sintered for 140 h at 1160 °C.

High-temperature XRD measurements were performed using a PANalytical MPD diffractometer equipped with an Anton Paar HTK1200 sample furnace and a curved-Johansson monochromator providing Cu $K\alpha_1$ radiation. A PIXcel detector was utilized and diffraction patterns were measured between 20° and 110° in 2θ, giving a range in Q of 1.4 to 6.7 $Å^{-1}$. Scans were measured for 3 h every 20 K from room temperature to 1090 K.

Powder neutron diffraction data were collected every 15 K between room temperature and 445 K on the high-resolution D2B diffractometer at the Institut Laue-Langevin, Grenoble, France. The wavelength of the neutron beam was 1.594 Å and the detector for the D2B diffractometer consisted of 128 ^{3}He counting tubes, spaced 1.25° apart. A full diffraction pattern between 5° and 165° in 2θ was recorded after moving the detector through 25 0.05° steps, giving a range between 1 and 7.6 $Å^{-1}$ in Q. A large sealed vanadium can containing 15 g of LT powder was used for the experiments and each scan was repeated 10 times to improve the counting statistics.

Rietveld refinements of the neutron and XRD data were performed using Topas Academic.[20] During these refinements, the occupancies of the atoms were fixed at their stoichiometric values and not refined. The wavelength and zero-offset for the room-temperature neutron measurements were refined using the lattice parameters from the room-temperature XRD measurements, giving a wavelength of 1.59333(1) Å. These were then fixed for all subsequent measurements and the lattice parameters refined as normal.

B. Computational

DFT calculations using the full-potential linear augmented plane-wave method (FP-LAPW) were carried out using the WIEN2 k code with the GGA introduced by Perdew *et al*.[21,22] For rhombohedral structures in the hexagonal cell WIEN2 k requires the atomic positions of the primitive rhombohedral 10-atom unit cell along with the hexagonal lattice parameters as the structural input. Muffin-tin radii of 1.69, 1.89, and 1.63 a_0 were used for the Li, Ta, and O atoms, respectively. A mixed basis consisting of the LAPW basis functions and localised orbitals was used inside the muffin-tin spheres and the Li $1s^2 2s^1$, Ta $5s^2 5p^6 4f^{14} 5d^3 6s^2$, and O $2s^2 2p^4$ were treated as valence states for the calculations.

The $R_{MT}K_{MAX}$ controls the size of the basis set used in the calculation and is determined by the muffin-tin radius of the smallest atom (R_{MT}) multiplied by the maximum reciprocal lattice vector allowed (K_{MAX}). The effect of the number of k-points and the $R_{MT}K_{MAX}$ on the convergence of the calculation and obtained n_e was investigated and 1000 k-points with an $R_{MT}K_{MAX}$ of 7 was subsequently used throughout, ensuring complete convergence with a reasonable time required for each calculation. This results in a basis size of roughly 1040 functions including local orbitals.

The OPTIC module in WIEN2 k was used for calculating the refractive indices. This code was produced by Ambrosch-Draxl and Sofo and allows the calculation of the imaginary parts of the dielectric tensor within the random-phase approximation.[23] The corresponding real parts of the dielectric tensor are obtained by Kramers-Kronig relations, which then allows the calculation of the refractive indices. A full description of the method and its integration into the FP-LAPW WIEN2 k code is given by Ambrosch-Draxl and Sofo.[23] For calculating the optical properties, an increased number of k-points was used (99999) and all the bands from the density of states were used in the calculation.

III. RESULTS

The lattice parameters as a function of temperature from Rietveld refinements of the XRD measurements are plotted in Figure 1 along with the residual of a linear fit to the *a* lattice parameter. There is a discontinuity in the lattice parameters at the phase transition to the paraelectric structure; this point is clear in the *c* lattice parameters and the plot of the residual of a linear fit to the *a* lattice parameter. These curves have been fitted with second- and fourth-order polynomials above and below the Curie point, respectively. The crossing point gives a Curie point for the LT powder of 927(3) K, which according to a study of the Curie point as a function of the Li concentration in LT[10] gives a composition of 49.7(1) mol. % Li_2O.

The change in the atomic positions, represented by the Megaw parameters, was calculated using Rietveld refinements of the neutron diffraction data measured between room temperature and 445 K. The Rietveld refinement of the diffraction data recorded at 300 K is shown in Figure 2. The calculated Megaw parameters from this refinement are given in Table I, along with the previously determined values by Megaw using single-crystal XRD measurements made by Abrahams and

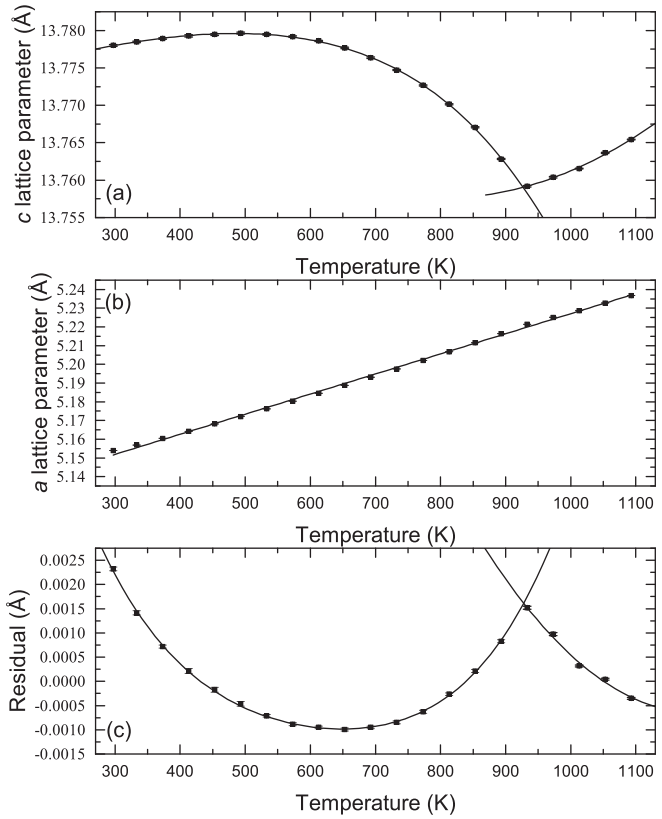

FIG. 1. The (a) *c* lattice parameter, (b) *a* lattice parameter, and (c) residual of a linear fit to the *a* lattice parameter as a function of temperature using XRD measurements. The *c* lattice parameter and residual of the linear fit to the *a* lattice parameter have been fitted with second- and fourth-order polynomials above and below the Curie point, respectively.

Bernstein on a stoichiometric LT crystal at 297 K.[12,24] The refined lattice parameters for the neutron measurements are included in Table II along with the background-corrected versions of the goodness of fit (GOF or χ^2), the weighted profile R-factor (R_{wp}), and R-factor (R_p) of the refinements.[25]

The calculated Megaw parameters are plotted as a function of temperature in Figure 3. The Ta displacement and tilt angle both decrease with increasing temperature, similar to

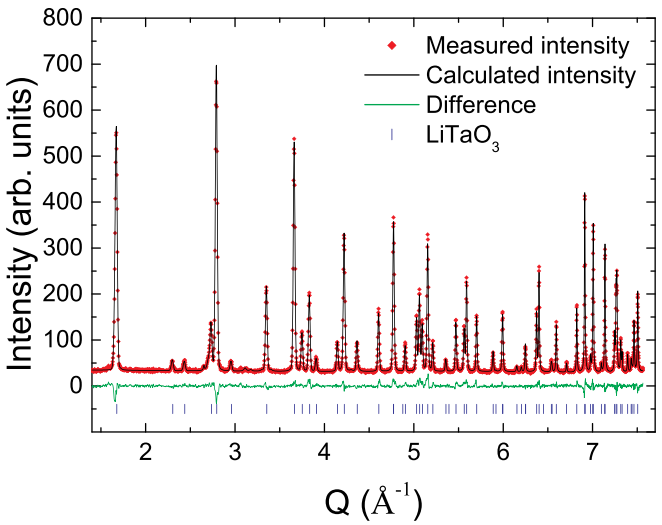

FIG. 2. Rietveld refinement of neutron diffraction measurement at 300 K.

TABLE I. Comparison between the determined Megaw parameters from this study and previous measurements.

	Displacement (Å)			
Source	Ta	Li	Octahedral distortion	Octahedral tilt (°)
Abrahams *et al.*[a]	0.20(1)	0.60(2)	−0.0026(2)	22.9(1)
This work	0.195(2)	0.601(4)	−0.0025(1)	22.98(2)

[a]Values determined by Megaw and Darlington using the single-crystal XRD measurements made by Abrahams and Bernstein at 297 K.[12,24]

LN. The Li displacement also decreases with increasing temperature. A linear fit to the octahedral distortion has been applied showing a small increase with increasing temperature. However, this trend is weak, with the errors in the calculated values being of the same order as the change in value across the temperature range investigated. The linear fits to the Ta displacement, Li displacement, and octahedral tilt are used to provide linear changes for use in the DFT calculations. The linear fits are valid in this temperature range; however, a nonlinear response may be evident if a greater temperature range was investigated.

DFT calculations were performed on the structures given by the linear fits to the Ta displacement, Li displacement, octahedral distortion, and octahedral tilt, which were calculated from the Rietveld refinements of the neutron diffraction measurements. A series of calculations were also performed only allowing the Li displacement, Ta displacement, octahedral tilt, or lattice parameters to vary. The octahedral distortion was kept fixed at the room-temperature value for these calculations. The calculated band gap varied from 3.91 eV at 300 K to 3.86 eV at 445 K.

The refractive indices at 550 nm were determined using the method developed by Ambrosch-Draxl and Sofo.[23] The resulting birefringence when all the properties were allowed to vary and when each was varied separately is plotted in Figure 4. The errors in the calculated values were estimated by comparing the results using the refined structures and those given by the linear fits in Figure 3. The calculated room-temperature birefringence is −0.030(2), which does not agree with the expected value of −0.005(1).[5] The calculated value is dependent on the band gap and is affected by its underestimation when using the GGA.[26]

TABLE II. Lattice parameters and fit criteria of the Rietveld refinements on neutron diffraction measurements.

Temperature (K)	$a = b$ (Å)	c (Å)	R_{wp}	R_p	GOF
300	5.1538(2)	13.776(1)	0.057	0.045	1.32
315	5.1550(2)	13.777(1)	0.058	0.045	1.35
330	5.1563(2)	13.776(1)	0.057	0.044	1.32
345	5.1575(2)	13.777(1)	0.057	0.045	1.32
360	5.1588(2)	13.777(1)	0.056	0.044	1.30
375	5.1601(2)	13.777(1)	0.057	0.045	1.32
390	5.1615(2)	13.778(1)	0.057	0.045	1.34
405	5.1629(2)	13.777(1)	0.055	0.044	1.30
425	5.1647(2)	13.778(1)	0.057	0.045	1.34
445	5.1665(2)	13.778(1)	0.058	0.046	1.36

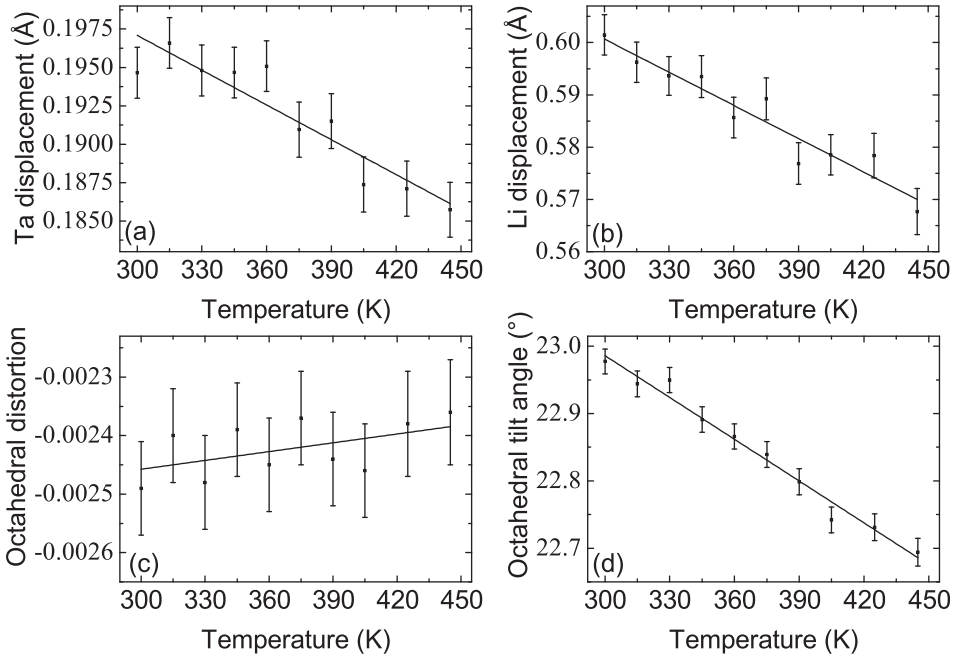

FIG. 3. The (a) Ta displacement, (b) Li displacement, (c) octahedral distortion, and (d) octahedral tilt angle as a function of temperature. Linear fits to the data are given by the black lines.

The birefringence increases with increasing temperature when all the atomic positions are varied, and the zero-birefringence point can be estimated by correcting the calculated room-temperature birefringence to the previously measured value of −0.005(1).[25] This gives a zero-birefringence temperature of 363(13) K, which agrees with the experimentally measured value of 373 K. The rescaled birefringence data are included in Figure S1 in the supplementary material. The change in the experimental birefringence measured between 300 and 373 K agrees with the calculated birefringence changes using the measured structural changes in this temperature range. This confirms that DFT calculations are sensitive to the small structural variations required to study the birefringence.

The calculated birefringence when only the Ta displacement, Li displacement, octahedral tilt, and lattice parameters are varied as a function of temperature, has also been plotted with linear fits. It is likely that the response in these calculations is non-linear; however, the linear fits are reasonable in the temperature range investigated. The change in the birefringence when only the Ta atoms are allowed to move is very similar to the response when all the atomic positions are varied, suggesting that the dominant effect on the optical properties of LT is the position of the Ta atom within the O octahedra. The changes in the octahedral tilt and Li displacement both result in a small increase in the birefringence with temperature, which is equal to the decrease given by the change in the lattice parameters. A trough at 368 K is visible in the calculated data when the Li displacement is changed, which is not seen in the other calculated values and is presumably an artifact caused by allowing only one atom to move.

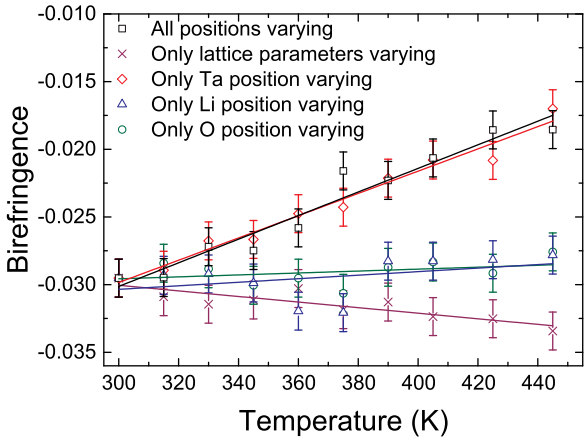

FIG. 4. Calculated birefringence values at 550 nm as a function of temperature when all parameters vary are given by the triangles. The values when only the Ta displacement, Li displacement, octahedral tilt, or lattice parameters are allowed to vary, are given by the diamonds, triangles, circles, and crosses, respectively. Linear fits to the data are given by the lines.

IV. CONCLUSIONS

The structural changes as a function of temperature have been confirmed to be the same as for those of LN; the Ta displacement and the octahedral tilt both decrease with increasing temperature. The use of neutron diffraction in this study has also shown a decrease in the Li displacement with increasing temperature. The results of the DFT calculations show that the displacement of the Ta from the centre of the O octahedra has the largest effect on the optical properties of LT. Changes in the Li displacement, octahedral tilt, and lattice parameters all have a small effect on the calculated birefringence.

The structure remains polar through the zero-birefringence point, with the small changes in the Ta displacement and octahedral tilt determining the change in the birefringence. This relationship may also help to explain the birefringence changes in mixed systems, for example, LN has a larger Nb displacement (0.28(1) Å) and as the LN content in LNT increases, the birefringence decreases resulting in a higher zero-birefringence temperature.[3,27,28]

There are a few examples of other materials that remain polar while going through an optically isotropic point, such as sodium bismuth titanate ($Na_{0.5}Bi_{0.5}TiO_3$, NBT) and some compositions of the mixed system between NBT and barium titanate ($BaTiO_3$, BT). This effect occurs as a result of a temperature or composition change; however, in these cases, the isotropy is related to rhombohedral to tetragonal phase transitions, and there is still debate about the nature of these transitions.[29,30]

The change in birefringence calculated from 300 to 445 K agrees well with the experimentally measured response of LT. This agreement shows that DFT calculations are sensitive to the small structural changes that occur as a function of temperature in these materials. However, precise structural measurements are required to investigate the structural origins of the physical properties. For example, in this study, the change in Li displacement, Ta displacement, octahedral distortion, and octahedral tilt between 300 and 445 K is of the same order as the uncertainties on the original room-temperature structure determined by Abrahams *et al*.

SUPPLEMENTARY MATERIAL

See supplementary material for Figure S1 showing the calculated birefringence rescaled to the room-temperature experimental value.

ACKNOWLEDGMENTS

We are grateful to the UK Engineering and Physical Sciences Research Council (EPSRC) for funding through Grant No. EP/F042787/1. The PANalytical MPD diffractometer used in this research was obtained through the Science City Energy Futures Project: Hydrogen Energy, with support from Advantage West Midlands (AWM). A. Bartasyte thanks the financial support of the Labex ACTION program (contract ANR-11-LABX-0001-01). We are grateful for experimental support from Dr. E. Suard (ILL).

[1]F. Shimura, J. Cryst. Growth **42**, 579 (1977).
[2]C. Baüumer, D. Berben, K. Buse, H. Hesse, and J. Imbrock, Appl. Phys. Lett. **82**, 2248 (2003).
[3]I. G. Wood, P. Daniels, R. H. Brown, and A. M. Glazer, J. Phys.: Condens. Matter **20**, 235237 (2008).
[4]A. M. Glazer, N. Zhang, A. Bartasyte, D. S. Keeble, S. Huband, and P. A. Thomas, J. Appl. Crystallogr. **43**, 1305 (2010).
[5]A. M. Glazer, N. Zhang, A. Bartasyte, D. S. Keeble, S. Huband, P. A. Thomas, I. Gregora, F. Borodavka, S. Margueron, and J. Hlinka, J. Appl. Crystallogr. **45**, 1030 (2012).
[6]M. Friedrich, A. Schindlmayr, W. G. Schmidt, and S. Sanna, Phys. Status Solidi B **253**, 683 (2016).
[7]K. Toyoura, M. Ohta, A. Nakamura, and K. Matsunaga, J. Appl. Phys. **118**, 64103 (2015).
[8]A. A. Ballman, H. J. Levinstein, C. D. Capio, and H. Brown, J. Am. Ceram. Soc. **50**, 657 (1967).
[9]P. F. Bordui, R. G. Norwood, C. D. Bird, and J. T. Carella, J. Appl. Phys. **78**, 4647 (1995).
[10]R. L. Barns and J. R. Carruthers, J. Appl. Crystallogr. **3**, 395 (1970).
[11]S. Kondo, K. Sugii, S. Miyazawa, and S. Uehara, J. Cryst. Growth **46**, 314 (1979).
[12]H. D. Megaw and C. N. W. Darlington, Acta Crystallogr. **A31**, 161 (1975).
[13]S. C. Abrahams, H. J. Levinstein, and J. M. Reddy, J. Phys. Chem. Solids **27**, 1019 (1966).
[14]H. D. Megaw, Acta Crystallogr. **A24**, 589 (1968).
[15]S. Cabuk, Int. J. Mod. Phys. B **24**, 6277 (2010).
[16]A. Riefer, S. Sanna, and W. G. Schmidt, in *Proceedings of ISAF-ECAPD-PFM 2012* (2012).
[17]C. Thierfelder, S. Sanna, A. Schindlmayr, and W. G. Schmidt, Phys. Status Solidi **7**, 362 (2010).
[18]S. Mamoun, A. E. Merad, and L. Guilbert, Comput. Mater. Sci. **79**, 125 (2013).
[19]A. Bartasyte, A. M. Glazer, F. Wondre, D. Prabhakaran, P. A. Thomas, S. Huband, D. S. Keeble, and S. Margueron, Mater. Chem. Phys. **134**, 728 (2012).
[20]A. A. Coelho, TOPAS Academic v4.1: General Profile and Structure Analysis Software for Powder Diffraction Data, 2007.
[21]P. Blaha, K. Schwartz, G. Madsen, D. Kvasnicka, and J. Luitz, *WIEN2 k, An Augmented Plane Wave plus Local Orbitals Program for Calculating Crystal Properties* (Vienna University of Technology, 2001).
[22]J. P. Perdew, K. Burke, and M. Ernzerhof, Phys. Rev. Lett. **77**, 3865 (1996).
[23]C. Ambrosch-Draxl and J. O. Sofo, Comput. Phys. Commun. **175**, 1 (2006).
[24]S. C. Abrahams and J. L. Bernstein, J. Phys. Chem. Solids **28**, 1685 (1967).
[25]B. H. Toby, Powder Diffr. **21**, 67 (2012).
[26]J. P. Perdew, Int. J. Quantum Chem. **28**, 497 (1985).
[27]S. C. Abrahams, J. M. Reddy, and J. L. Bernstein, J. Phys. Chem. Solids **27**, 997 (1966).
[28]S. C. Abrahams, W. C. Hamilton, and J. M. Reddy, J. Phys. Chem. Solids **27**, 1013 (1966).
[29]S. Gorfman, A. M. Glazer, Y. Noguchi, M. Miyayama, H. Luo, and P. A. Thomas, J. Appl. Crystallogr. **45**, 444 (2012).
[30]B. W. Lee, J.-H. Ko, X. Li, and H. Luo, J. Korean Phys. Soc. **66**, 1350 (2015).